

## Indirect, quasidirect, and direct optical transitions in the pseudomorphic $(4 \times 4)$ -monolayer Si-Ge strained-layer superlattice on Si(001)

R. People and S. A. Jackson

*AT&T Bell Laboratories, Murray Hill, New Jersey 07974*

(Received 6 April 1987; revised manuscript received 26 May 1987)

Estimates are presented for the lower-lying optical transitions in the pseudomorphic  $(4 \times 4)$ -monolayer Si-Ge strained-layer superlattice on Si(001). These lower-lying  $q=0$  superlattice transitions tend to cluster into groups having energy centroids near 0.76, 1.03, 1.2, 1.6, and 2.3 eV, for light polarized in the plane of the interface. The transitions near 0.76 and 1.03 eV are indirect. Transitions near 1.2 and 1.6 eV arise from zone-folded bulklike bands and have a partially direct character, whereas the transitions near 2.3 eV are strictly direct. Surface steps and inter-valley phonons would tend to relax the in-plane ( $\mathbf{k}_{\parallel}$ ) momentum conservation rule, and thus allow zone-folded quasidirect character transitions near 0.76 eV.

There is considerable interest at present in ultrathin pseudomorphic heterostructures of Ge and Si, stimulated in part by (i) evidence for a strain-induced order-disorder transition in (Ge, Si) alloys,<sup>1</sup> (ii) determination of the maximum (critical) layer thickness for pure Ge on Si,<sup>2</sup> and (iii) predictions of zone-folding induced quasidirect gap optical transitions in the (Ge, Si) system.<sup>3-5</sup> Zone-folding effects are expected to occur when the periodicity of a superstructure equals an integral number of bulk lattice constants. In the case of Ge and Si, which crystallize in the cubic diamond structure, one lattice constant is composed of four monolayers along  $\langle 001 \rangle$  directions. It is therefore apparent that the alternating four-monolayer [hereafter denoted as the  $(4 \times 4)$  monolayer] Si-Ge heterostructure is the most likely candidate of the pseudomorphic monolayer structures which should exhibit zone-folding induced modifications of the superlattice band structure.

In the present Rapid Communication, estimates are given of the lower-lying optical-transition energies for the  $(4 \times 4)$ -monolayer Si-Ge strained-layer superlattice. These results were stimulated in part by recent electro-reflectance measurements on this strained-layer heterostructure,<sup>6</sup> indicating the occurrence of direct-character, superlattice optical transitions at energies of 0.76, 1.25, and 2.31 eV. These direct-character transitions are characteristic of neither the cubic Si or the coherently strained Ge. We use an effective-mass envelope-function model to calculate of the lower-lying superlattice optical transitions, incorporating the effects of coherency strain, and assuming continuity of the one-dimensional wave function,  $f(z)$ , and  $m^{-1}(df/dz)$ , as outlined by Bastard and Brum.<sup>7</sup> We find superlattice optical transitions which tend to cluster near 0.76, 1.03, 1.2, 1.6, and 2.3 eV (for light polarized in the plane of the interface). It is shown that the transitions near 1.2 to 2.3 eV have some direct character. However, the transitions near 0.76 and 1.03 eV are indirect, since they arise from bulk extrema which are either unaffected by the superlattice potential or which are folded but not into the zone center.

A full self-consistent interface calculation (SCIC) of the ground-state properties of the  $(4 \times 4)$ -monolayer

structure has shown that charge densities and potentials within this supercell are identical to those of cubic bulk Si and strained bulk Ge, except for a transition region confined to one monolayer on either side of the heterointerface.<sup>8</sup> This result is extremely important in that it implies that no new crystal structure is formed in the  $(4 \times 4)$ -monolayer superlattice, and further that the respective material components may be characterized by their associated bulk parameters. In light of these results, superlattice potential diagrams may be established by use of the bulk band extrema energies of cubic Si and phenomenological deformation potential estimates of the strained band edges for Ge,<sup>9-11</sup> along with the SCIC results for the valence-band offset.<sup>8,12</sup>

We have considered band extrema associated with the  $\Gamma_{25}^{\prime}$  valence-band along with the  $\Gamma_{2}^{\prime}$  and  $\Gamma_{15}$  conduction bands for the cubic Si and coherently strained Ge. In general, strain and spin-orbit effects induce numerous splittings of these extrema. The question of which states may act as barriers for a given well state is determined by requiring that (i) in-plane crystal momentum ( $\mathbf{k}_{\parallel}$ ) is conserved, and (ii) wave-function overlap between barrier and well states is allowed by symmetry. The latter issue is readily addressed using elementary-group theoretic techniques.

For a superlattice potential along  $\langle 001 \rangle$ , the six lowest Si conduction-band minima,  $\text{Si}(\Delta_1^{[6]})$ , may be grouped into two classes. The first class consists of the two valleys along  $\langle 001 \rangle$  in momentum space,  $\text{Si}(\Delta_1^{\pm})$ , while the second class consists of the four (in-plane) valleys normal to  $\langle 001 \rangle$ ,  $\text{Si}(\Delta_1^{\parallel})$ . Similar considerations apply for the  $X$  points. In the case of the  $(4 \times 4)$ -monolayer superlattice (having period  $\approx 2a_0$ ) the bulk band structure along  $\langle 001 \rangle$  experiences a single folding approximately midway between the  $\Gamma$  and  $X$  symmetry points as illustrated in Fig. 1. Single-group representatives associated with cubic Si are used for identification purposes only. Note that at  $\mathbf{k} \sim 0.7$  the distance between  $\Gamma$  and  $\bar{X}$  the zone-folded  $\Delta_2^{\prime}$  band (solid curve) would intersect the not yet folded  $\Delta_1$  band originating from  $\Gamma_{15}$ . Although such an intersection is allowed under cubic symmetry, it is strictly forbidden under the reduced ( $C_{2v}$ ) symmetry associated with the  $\Delta$

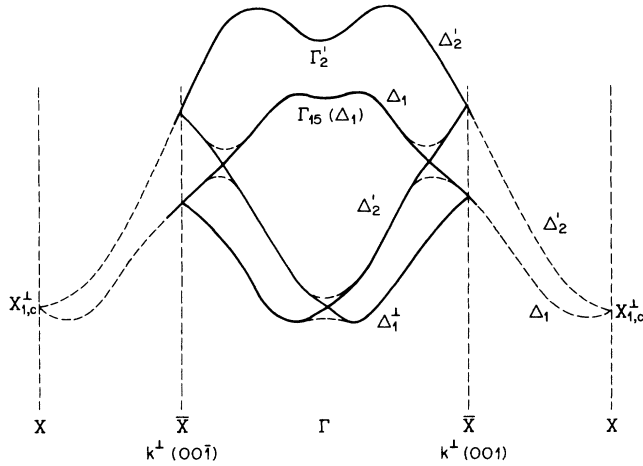


FIG. 1. Schematic of a single folding of the bulk conduction bands of cubic Si.  $X$  and  $\bar{X}$  denote the (001) Brillouin-zone boundary of Si in the bulk and under the superlattice potential, respectively.

direction for the  $(4 \times 4)$  strained-layer superlattice. Indeed  $\Delta_1$  and  $\Delta_2$  both transform as the totally symmetrical ( $A_1$ ) representation of  $C_{2v}$ . Note that the zone-folded  $\text{Si}(\Delta_1^\perp)$  bands have extrema near, but not at,  $\mathbf{k}=\mathbf{0}$ . The four in-plane  $\text{Si}(\Delta_1^\parallel)$  valleys will be unaffected by the (001) superlattice potential, so that their conduction-band minima have large  $\mathbf{k}$  [ $\sim 0.9\mathbf{k}(X)$ ], as illustrated in Fig. 2. When estimating superlattice energies we assume that the various Si-folded and non-zone-folded conduction-band extrema are initially degenerate. The lowest conduction-band minima of the coherently strained Ge are also derived from  $\Delta_1$ -conduction states,<sup>11</sup> and may be grouped into the two classes previously described for Si. One major difference exists, however; namely, the coherency strain splits the  $\text{Ge}(\Delta_1^\perp)$  and  $\text{Ge}(\Delta_1^\parallel)$  extrema by approximately 0.7 eV, with the  $\text{Ge}(\Delta_1^\parallel)$  lying lowest in energy.

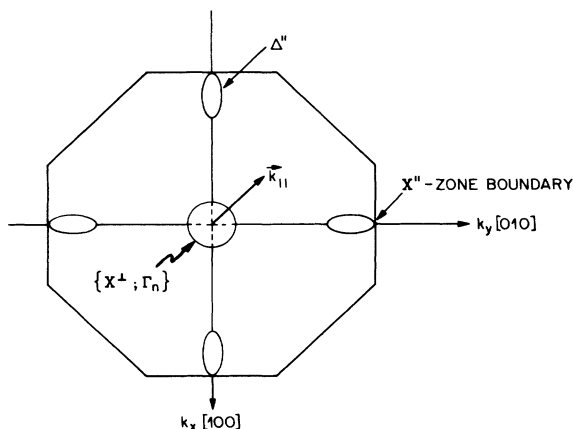


FIG. 2. (001) surface Brillouin zone for cubic Si and coherently strained Ge on (001) Si.

The in-plane crystal momentum associated with the various band extrema is readily obtained by considering the projected two-dimensional Brillouin zone of the superlattice as shown in Fig. 2. All zone-folded  $X_1^\perp$  conduction states are assumed projected onto  $\mathbf{k}=\mathbf{0}$ ;  $\Delta_1^\perp$  states are folded to a point near but not at  $\mathbf{k}=\mathbf{0}$ , whereas the in-plane  $\Delta_1^\parallel$  and  $X_1^\parallel$  states retain wave vectors  $\mathbf{k} \sim 0.9\mathbf{k}(X)$  and  $\mathbf{k}(X)$ , respectively. Due to the  $k_\parallel$  conservation rule, it is apparent that the  $\text{Ge}(\Delta_1^\parallel)$  states can act as a barrier for the  $\text{Si}(\Delta_1^\parallel)$  states only, and further that the corresponding superlattice conduction states have large  $\mathbf{k}$  values. A number of allowed couplings between the direct and/or zone-folded conduction-band extrema are shown in Fig. 3, under the  $D_{2d}$  superlattice symmetry at the  $\Gamma$  point ( $T=300$  K). The energy positions of the various extrema shown in Fig. 3 reflect a valence-band offset in which the upper  $(\frac{3}{2}, \pm \frac{3}{2})$  valence-band edge of Ge lies 0.84 eV higher than the Si ( $J = \frac{3}{2}$ ) valence-band edge. Spin-orbit effects have been included in these estimates.<sup>12</sup> It should be noted that the coherency strain completely decouples the  $J = \frac{3}{2}$  valence-band edge of Ge.<sup>8-11</sup> The barrier heights and confinement energies for the various conduction- and valence-band superlattice potentials are listed in Table I. Mass parameters used are measured values where available or calculated  $\mathbf{k} \cdot \mathbf{p}$  curvatures.<sup>13-15</sup> Extrema energies in the unstrained bulk materials are given in Ref. 16.

In brief, we find that the  $q=0$  (lower-bound) energy for the superlattice subband associated with the  $\text{Ge}(\Delta_1^\parallel)$  barrier and the  $\text{Si}(\Delta_1^\parallel)$  well, denoted by  $E_e^{(0)}(\Delta_1^\parallel)$ , lies 0.06 eV above the  $\text{Si}(\Delta_1^{[6]})$  conduction-band edge (see Fig. 3). The  $q = \pm \pi/d$  solution (which defines the subband width) lies above the  $\text{Ge}(\Delta_1^\parallel)$  band edge. This result was obtained assuming an in-plane well and barrier electron masses are given by the conductivity effective masses for Si and Ge; i.e.,  $0.26m_0$  and  $0.12m_0$ , respectively. In like manner the zone-folded  $\text{Ge}(\Delta_1^\perp)$  band edge forms a barrier of 0.765-eV height for the  $\Delta_1^\perp$  electrons in Si (Fig. 2) giving rise to the subband denoted  $E_e^{(0)}(\Delta_1^\perp)$ , whose  $q=0$  (lower-bound) energy lies 0.32 eV above the  $\text{Si}(\Delta_1^{[6]})$  conduction-band edge. The width of the  $E_e^{(0)}(\Delta_1^\perp)$  subband is  $\approx 0.17$  eV. The  $\text{Ge} \Gamma_2'$  and  $X_1^\perp$  states are nearly degenerate. Both these states act as a barrier for the zone-folded quasidirect  $\text{Si}(X_1^\perp)$  state and give rise to a superlattice state 0.38 eV above the  $\text{Si}(X_1^\perp)$  band edge. The  $B_2$  component of the  $\text{Ge}(\Gamma_{15})$  states also forms a barrier for the  $\text{Si}(X_1^\perp)$  state of 2.37 eV height. This gives rise to the subband denoted  $E_e^{(0)}\{\text{Si}(X_1^\perp), \Gamma_{15}\}$  at 0.79 eV above the  $\text{Si}(X_1^\perp)$  band edge and having a miniband width of 0.14 eV.

The  $\text{Si}(\Gamma_2')$  state forms a barrier for both the  $\text{Ge}(\Gamma_2')$  and the nearly degenerate zone-folded  $\text{Ge}(X_1^\perp)$  state. The energy position of the  $\text{Si}(\Gamma_2')$  barrier relative to the  $\text{Ge}(\Gamma_2')$  well is based upon our estimate that the  $\Gamma_2'$  band gap for the strained Ge is 1.175 eV, for growth on  $\text{Si}(001)$ . We have used the measured  $\text{Ge}(\Gamma_2')$  mass  $0.04m_0$  along with an assumed  $\text{Si}(\Gamma_2')$  barrier mass of  $0.64m_0$ . The  $\Gamma_2'$  superlattice potential gives rise to a bound state at 0.76 eV above the  $\text{Ge}(\Gamma_2')$  band edge, having a miniband width  $\sim 0.24$  eV. Therefore a set of direct transitions at energies of 2.30 and 2.41 eV are obtained

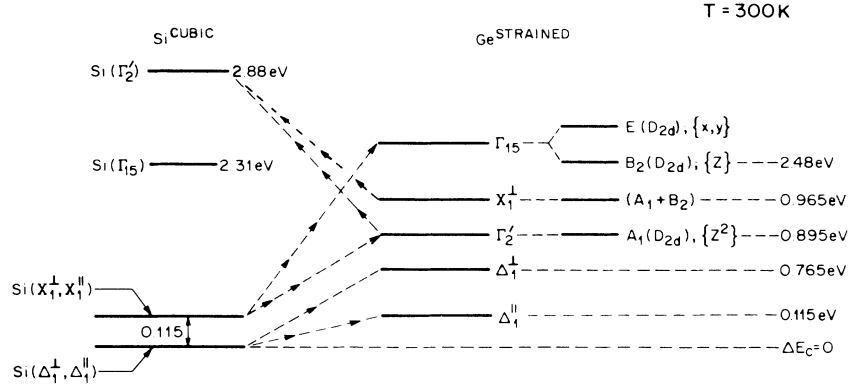


FIG. 3. A number of symmetry allowed couplings under  $D_{2d}$  superlattice symmetry at the  $\Gamma$  point, for  $\Gamma_{15}$ ,  $\Delta_1$ , and  $X$  conduction states;  $T = 300$  K.

for light polarized in the plane of the layers. Corresponding transitions for the  $\text{Ge}(X_1^+)$  well lie  $\sim 0.04$  eV higher in energy.

Calculated superlattice optical transition energies are listed in Table II. We also list the character of these transitions along with the decay length of the associated conduction state. Note that the transition near 1.6 eV is strongly localized within the Si quantum well, whereas the  $X_1^+$  component at 1.2 eV and the  $\Gamma_2'$  transition at 2.30 eV are only partially localized with the respective Si and Ge well layers. If we denote the superlattice-induced  $\Gamma$  character of a zone-folded conduction state as  $\beta$ , then  $\beta \sim [\langle \phi(\Gamma_2') | V_{\text{SL}} | \phi(X) \rangle] / \Delta E_{\Gamma-X}$ . Here  $\phi$  denotes bulk conduction wave functions of specified wave vector,  $V_{\text{SL}}$  the  $\langle 001 \rangle$  superlattice potential, and  $\Delta E_{\Gamma-X}$  the energy separation between the  $\Gamma_2'$  and  $X$  bulk band extrema. Fourier expansion of  $V_{\text{SL}}$  in terms of the superlattice zone-boundary wave vector  $\vec{G}$ , shows that the dominant contribution to the matrix element in  $\beta$  arises from the term  $V_{\text{SL}}^{(1)} \exp(i\vec{G} \cdot \mathbf{r})$ . Since  $V_{\text{SL}}^{(1)} \sim 2V_0/3\pi \sim 2\Delta E_g/3\pi$  and  $\Delta E_{\Gamma-X} \sim 2$  eV, we see that  $\beta \sim 0.1$  for a band-gap difference  $\Delta E_g \sim 1$  eV (as applies in the present case). The quantity we call the relative absorptance is a rough estimate of the relative oscillator strength for a vertical (no-phonon) transition at  $\mathbf{k} = \mathbf{0}$ . Assuming an estimated 10% superlattice-induced  $\Gamma$  character in a zone-folded (well or barrier) state,<sup>5,15</sup> the quantity given is then the square of the product of the  $\Gamma$ -state character in the well

and barrier states. Since phonon-assisted processes are ignored, the relative absorptance of the  $\Delta_1^+$  and  $\Delta_1^{\parallel}$  states remains indeterminant. Uncertainties in transition energies  $\sim \pm 50$  meV are expected, originating primarily from combined uncertainties in the strained band gaps<sup>9,11</sup> and valence-band offsets.<sup>8,12</sup> Note that a factor of 2 increase in mass parameters gives rise to changes in the  $E_e^{(0)}(\Delta_1^{\parallel})$  and  $E_e^{(0)}(\Delta_1^+)$  confinement energies  $\sim 0.003$  and  $0.030$  eV, respectively, indicating that the binding energy of these states are rather insensitive to the mass parameters used. In like manner, increasing the  $\text{Ge}(\Gamma_2')$  well mass by a factor of 2.5 (to  $0.10m_0$ ) results in a decrease of the  $E_e^{(0)}(\Gamma_2')$  confinement energy by 0.015 eV.

In summary, we have calculated a number of lower-lying optical-transition energies (for light polarized in the plane of the layers) in the  $(4 \times 4)$ -monolayer Si-Ge strained-layer superlattice on Si(001). These results reflect a full self-consistent calculation of the ground-state electronic properties of the  $(4 \times 4)$ -monolayer supercell, and in particular reflect the bulklike character of the superlattice constituents.<sup>8</sup> Calculated direct-character transitions near 1.2 and 1.6 eV are identified with weakly and strongly localized zone-folded states in the Si layers confined by the  $\text{Ge}(\Gamma_2', X_1^+)$  and  $\text{Ge}(\Gamma_{15})$  conduction-band edges, respectively. Transitions near 2.35 eV are identified with the lowest totally direct superlattice transition, arising from  $\Gamma_2'$  bulk states. Two other sets of indirect transitions centered near 0.76 and 1.03 eV are also pre-

TABLE I. Parameters used in calculating  $q=0$  subband energies for the  $(4 \times 4)$ -monolayer Si-Ge strained-layer superlattice. All energies are relative to the bottom of the associated well.

Subband designation	Well parameters		Barrier parameters		Subband energy (eV)
	$m^*/m_e$	Width (Å)	Height (eV)	$m^*/m_e$	
$E_h^{(0)}(\frac{3}{2}, \pm \frac{3}{2})$	0.21	5.8	0.84	0.49	0.37
$E_h^{(0)}(\frac{1}{2}, \pm \frac{1}{2})$	0.067	5.8	0.69	0.16	0.32
$E_e^{(0)}(\Delta_1^{\parallel})$	0.26	5.43	0.115	0.12	0.06
$E_e^{(0)}(\Delta_1^+)$	0.98	5.43	0.765	0.53	0.32
$E_e^0\{\text{Si}(X_1^+), (\Gamma_2', X_1^+)\}$	0.50	5.43	(0.78, 0.85)	(0.04, 0.5)	0.38
$E_e^0\{\text{Si}(X_1^+), \Gamma_{15}\}$	0.50	5.43	2.37	0.53	0.79
$E_e^{(0)}(\Gamma_2')$	0.04	5.8	1.99	0.64	0.76

TABLE II. Lowest-energy  $q=0$  superlattice optical transitions for the  $(4\times 4)$ -monolayer Si-Ge strained-layer superlattice on Si(001), for light polarized in  $(x,y)$  plane. VB and CB mean valence-band and conduction-band states, respectively.

	Conduction-band state				
	$E_e^{(0)}(\Delta_{\parallel}^{\uparrow})$	$E_e^{(0)}(\Delta_{\perp}^{\uparrow})$	$E_e^{(0)}\{\text{Si}(X_{\perp}^{\uparrow}), (\Gamma_{2'}^{\uparrow}, X_{\perp}^{\uparrow})\}$	$E_e^{(0)}\{\text{Si}(X_{\perp}^{\uparrow}), \Gamma_{13}\}$	$E_e^{(0)}(\Gamma_{2'}^{\uparrow})$
$(\frac{3}{2}, \pm \frac{1}{2})$ VB (eV)	0.71	0.97	1.15	1.56	2.30
$(\frac{3}{2}, \pm \frac{1}{2})$ VB (eV)	0.82	1.08	1.26	1.67	2.41
Character	Indirect	ZF indirect	Quasidirect	Quasidirect	Direct
CB state decay length (Å)	24.0	4.0	(15.3,4.3)	2.13	4.86
Relative absorptance	...	...	$10^{-2}$	$10^{-2}$	$\equiv 1.0$

dicted. In the absence of intervalley coupling interactions the transitions centered near 0.76 eV are indirect and arise entirely from non-zone-folded bulk bands. Possible intervalley coupling mechanisms include (i) intervalley phonon scattering<sup>17,18</sup> and (ii) the presence of surface steps, which destroy the in-plane translational symmetry, thus relaxing the  $\mathbf{k}_{\parallel}$  conservation rule. Intervalley phonon scattering does not appear to be very plausible in view of the fact that the superlattice states involved in such couplings are widely separated in energy in comparison to  $k_B T$  at room temperature. The presence of  $\pm 1$ -monolayer surface steps, however, would relax the in-plane  $\mathbf{k}_{\parallel}$ -conservation rule. Note that the zone-folded  $\text{Si}(X_{\perp}^{\uparrow})$  state is degenerate with the  $\text{Ge}(\Delta_{\parallel}^{\uparrow})$  state, as

shown in Fig. 3. In the absence of  $\mathbf{k}_{\parallel}$  conservation these states would mix strongly, thus giving rise to a quasidirect superlattice transition near 0.8 eV. Further, such surface steps give rise to an overlap in the  $(\frac{3}{2}, \pm \frac{1}{2})$  and  $(\frac{3}{2}, \pm \frac{1}{2})$  valence-subband levels, resulting in a distribution of initial states having an energy width  $\sim 0.2$  eV. This is highly suggestive in view of the  $\sim 0.2$  eV measured width of all superlattice-related transitions given in Ref. 6.

We would like to acknowledge the encouragement of V. Narayanamurti, P. A. Fleury, and A. Y. Cho during the course of these studies. Helpful discussions with Mark Hybertsen, T. P. Pearsall, J. Bevk, and M. Schluter are gratefully acknowledged.

- <sup>1</sup>A. Ourmazd and J. C. Bean, Phys. Rev. Lett. **55**, 765 (1985).  
<sup>2</sup>J. Bevk, J. P. Mannaerts, L. C. Feldman, B. A. Davidson, and A. Ourmazd, Appl. Phys. Lett. **49**, 286 (1986).  
<sup>3</sup>U. Gnutzmann and K. Clausecker, Appl. Phys. **3**, 9 (1974).  
<sup>4</sup>J. A. Moriarty and S. Krishnamarthy, J. Appl. Phys. **54**, 1892 (1983).  
<sup>5</sup>S. A. Jackson and R. People, Mater. Res. Soc. Symp. Proc. **56**, 365 (1986).  
<sup>6</sup>T. P. Pearsall, J. Bevk, L. C. Feldman, A. Ourmazd, J. M. Bonar, and J. P. Mannaerts, Phys. Rev. Lett. **58**, 729 (1987).  
<sup>7</sup>G. Bastard and J. A. Brum, IEEE J. Quantum Electron. **QE-22**, 1625 (1986).  
<sup>8</sup>C. G. Van de Walle and R. M. Martin, J. Vac. Sci. Technol. B **3**, 1256 (1985).  
<sup>9</sup>R. People, Phys. Rev. B **32**, 1405 (1985).  
<sup>10</sup>D. V. Lang, R. People, J. C. Bean, and A. M. Sergent, Appl.

- Phys. Lett. **47**, 1333 (1985).  
<sup>11</sup>R. People, J. C. Bean, and D. V. Lang, in *Proceedings of the 18th International Conference on the Physics of Semiconductors*, edited by O. Engström (World Scientific, Singapore, 1987), p. 767.  
<sup>12</sup>C. G. Van de Walle and R. M. Martin, in *Proceedings of the Conference on the Physics of Compound Semiconductor Interfaces* [J. Vac. Sci. Technol. B **4**, 1055 (1986)].  
<sup>13</sup>J. C. Hensel and K. Suzuki, Phys. Rev. B **9**, 4219 (1974).  
<sup>14</sup>H. Hasegawa, Phys. Rev. **129**, 1029 (1963).  
<sup>15</sup>G. Dresselhaus and M. S. Dresselhaus, Phys. Rev. **160**, 649 (1967).  
<sup>16</sup>J. R. Chelikowsky and M. L. Cohen, Phys. Rev. B **14**, 556 (1976).  
<sup>17</sup>D. Long, Phys. Rev. **120**, 2024 (1960).  
<sup>18</sup>M. J. Kelly and W. Hanke, Phys. Rev. B **23**, 924 (1981).